

Magneto Optical and Microstructural Investigation of Grain Boundaries in Large Grain High Purity Niobium for Superconducting RF Cavities

P. J. Lee, A. A. Polyanskii (*Magneto Optical Imaging*), Z. H. Sung (*TEM, EELS*), A. Gurevich, D. C. Larbalestier

Applied Superconductivity Center, National High Magnetic Field Laboratory - FSU

C. Antoine, P. C. Bauer*, C. Boffo, and H. C. Edwards

Fermilab

**now at ITER*



Single Crystal Niobium
Technology Workshop

CBMM

Araxá, Brazil

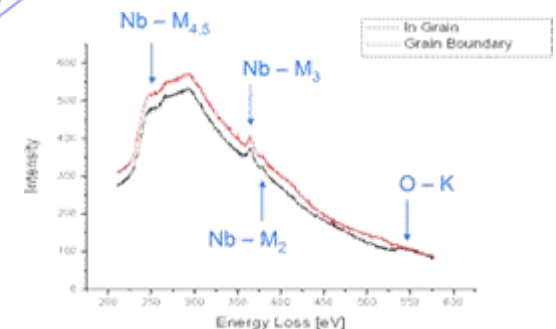
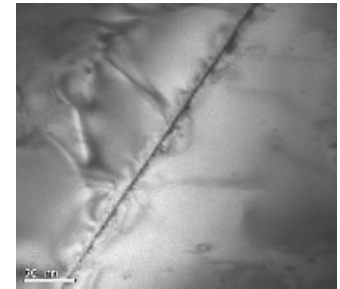
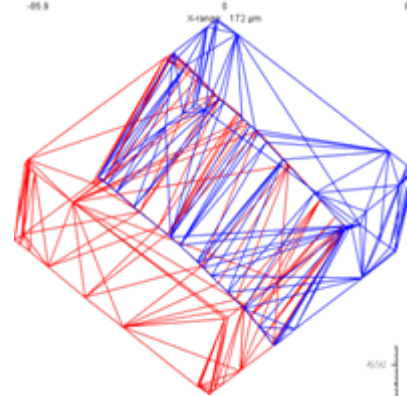
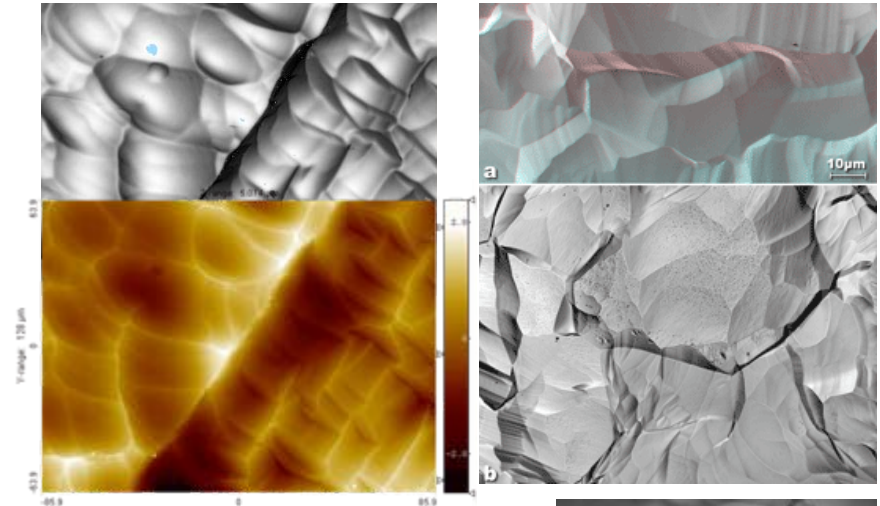
Oct. 30 — Nov. 1, 2006

Possible Sources of Cavity Degradation

🌐 Surface Topology/Debris

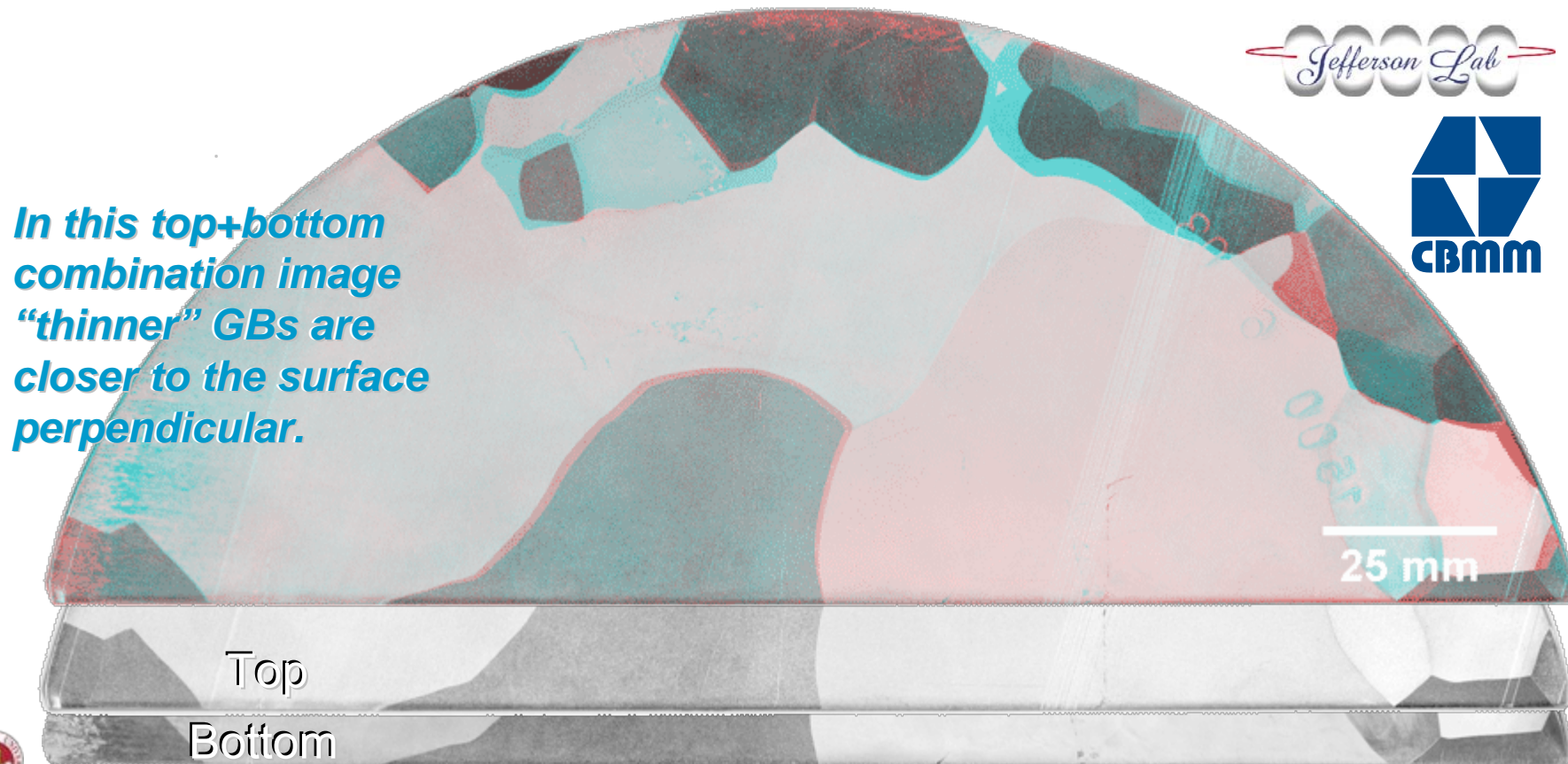
🌐 Microstructure

🌐 Chemistry



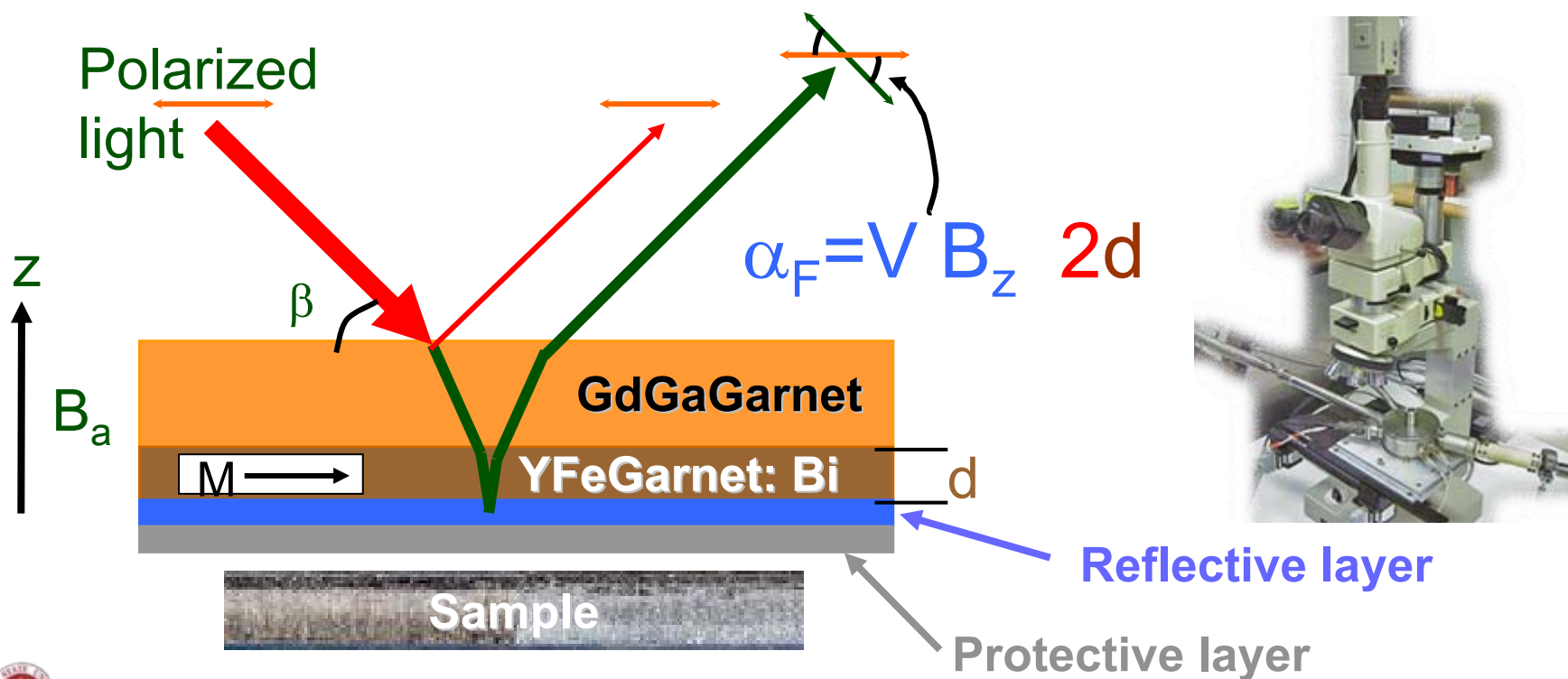
Large Grain **CBMM** Slice from JeffersonLab as Test-bed

- Allows testing of individual microstructural features through-processing



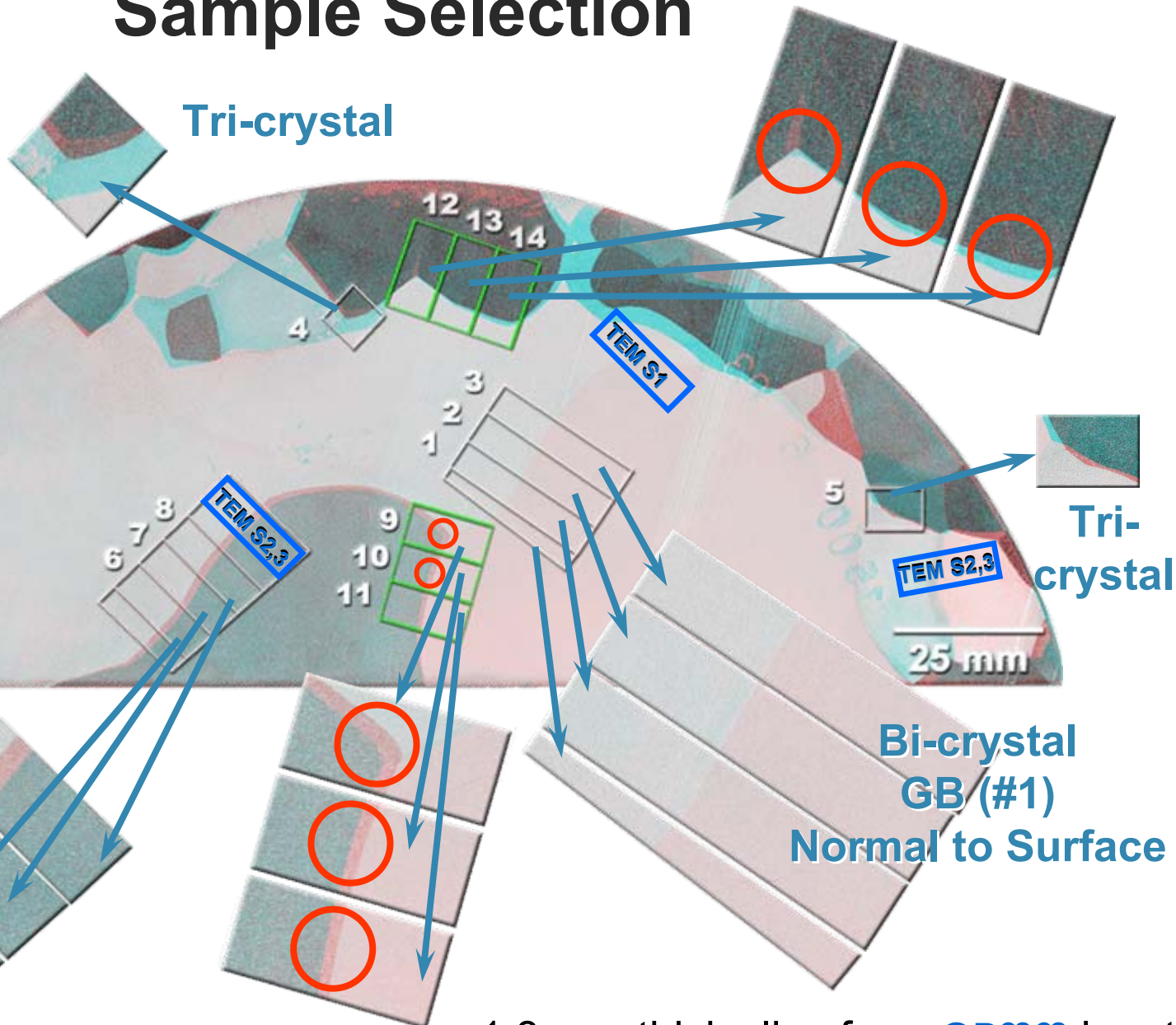
Magneto Optical Imaging: Allows Direct Imaging of B_z in Plane Above Sample

Double Faraday effect occurs in reflective mode using Bi-doped YIG indicator film with in-plane magnetization



Sample Selection

In this top+bottom combination image "thinner" GBs are closer to the surface perpendicular



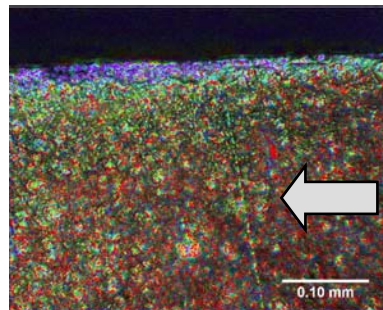
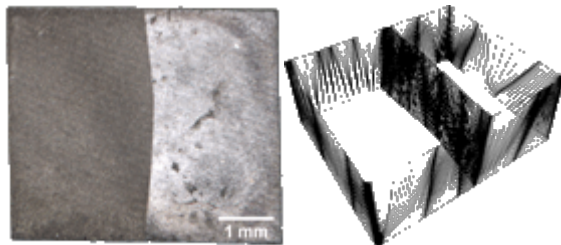
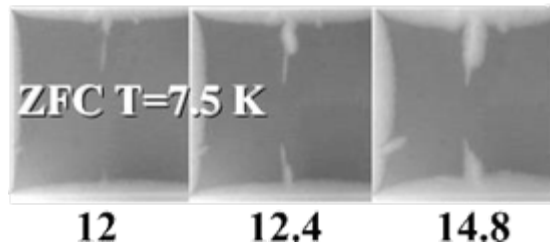
Bi-crystal GB (#2)
~30° to Surface

Bi-crystal GB (#1)
Normal to Surface

1.8 mm thick slice from **CBMM** ingot



Previously (SRF'05 – Physica C)

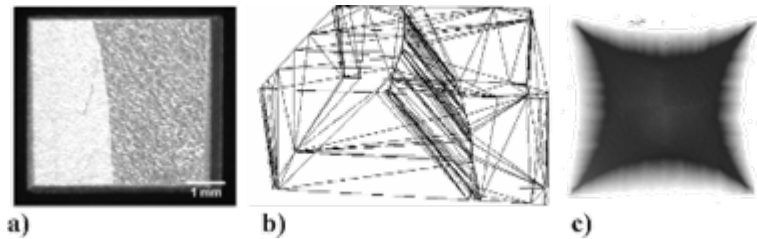


Depth Map,
5 μm Range

- Examination of 2 bi-crystals and 2 tri-crystals showed premature flux penetration at only one grain boundary in one sample (perpendicular magnetic field).
- Flux penetrated grain boundary was parallel to external magnetic field.
- Topology did not appear to be a factor in this case (the non-penetrated GBs had larger surface steps than the penetrated GB).

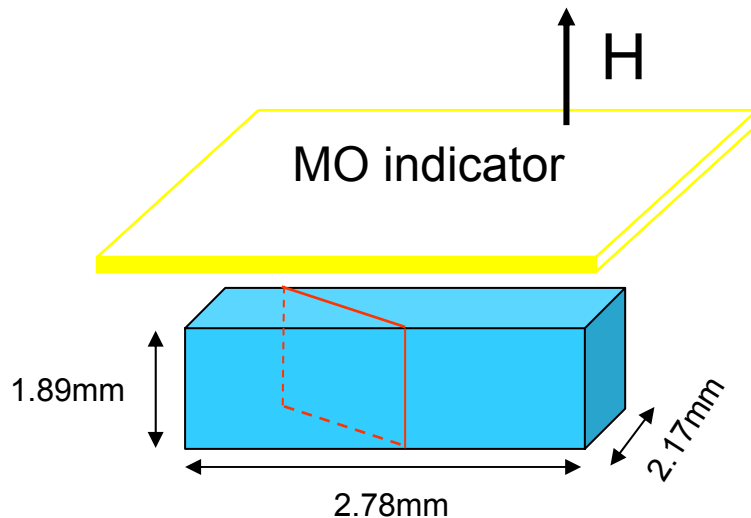


Experiment 1: Vary GB Angle to Surface

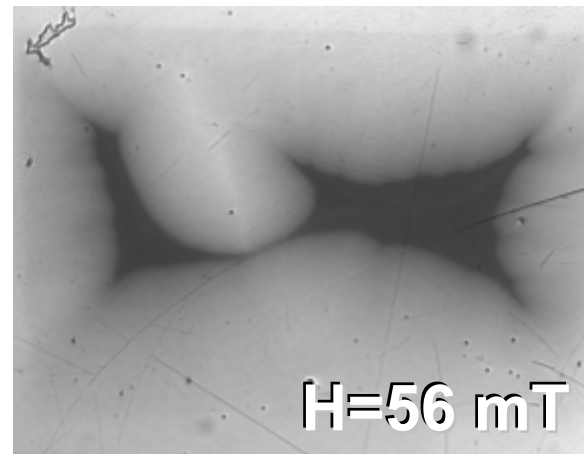
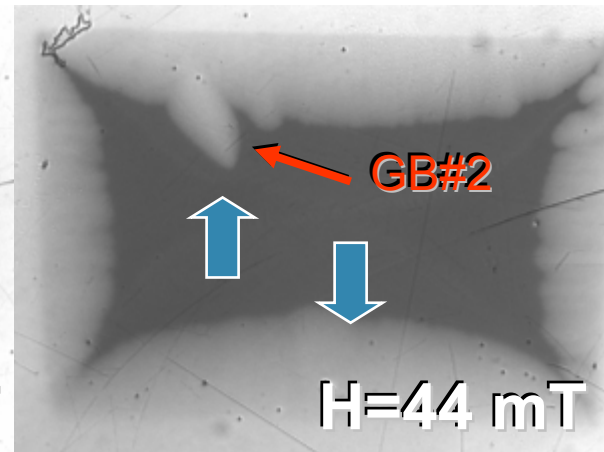
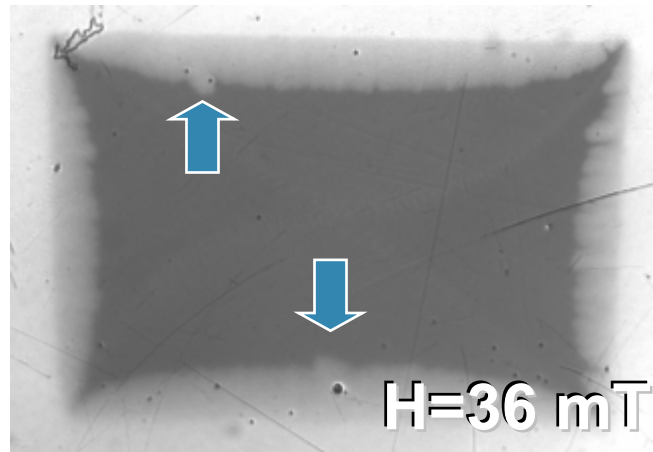
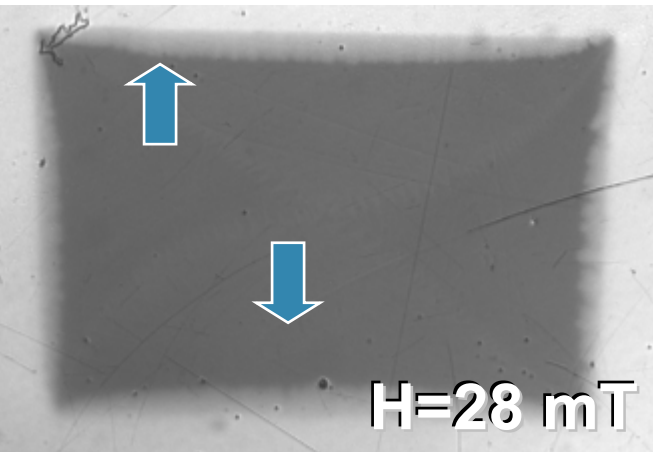
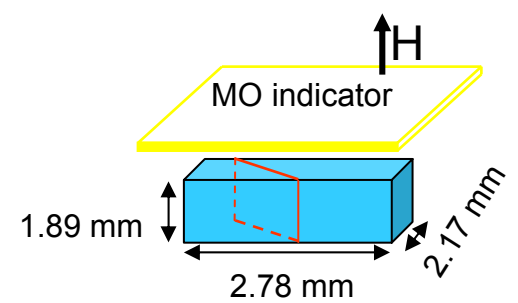


Take sample with grain boundary at 35° to surface – that did not show flux penetration at GB in earlier MO.

Rotate and re-slice sample so that the GB is now perpendicular to the top surface.



Magnetic flux now penetrates (magnetic field parallel to plane of GB).



But note: asymmetric penetration.

1 mm



Thickness of sample is 1.89 mm

Polyanskii

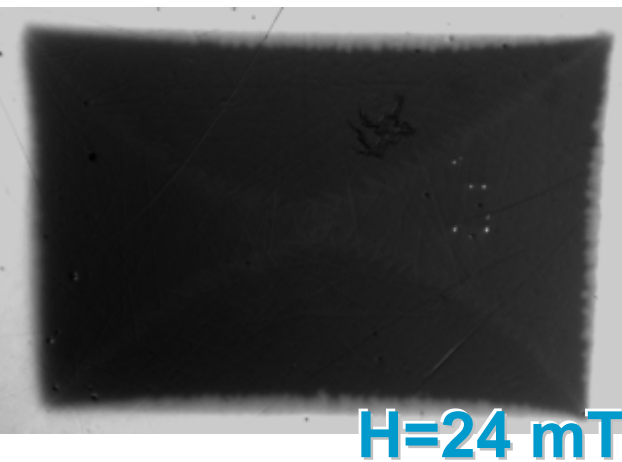
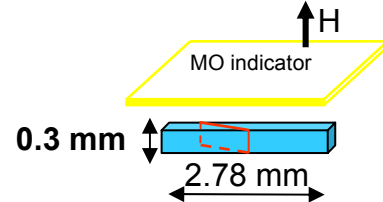


Experiment 2: Grain Boundary Orientation Sensitivity

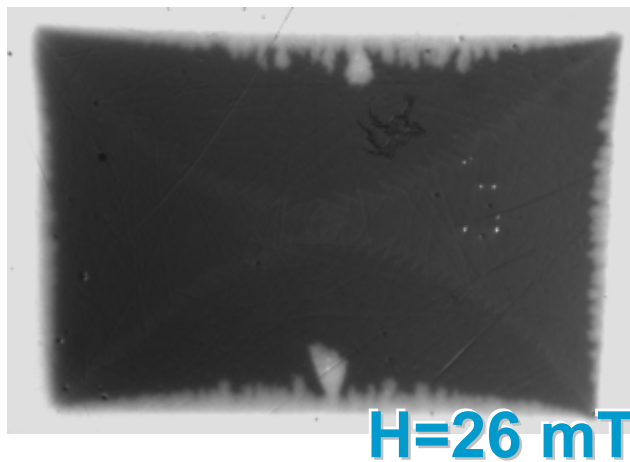
- 🌐 What happens when the GB is not planar but twists through the sample?
 - 🌐 Does this make the penetration asymmetric?
- 🌐 Test: slice the specimen once more to reduce thickness and top-to-bottom grain boundary displacement.



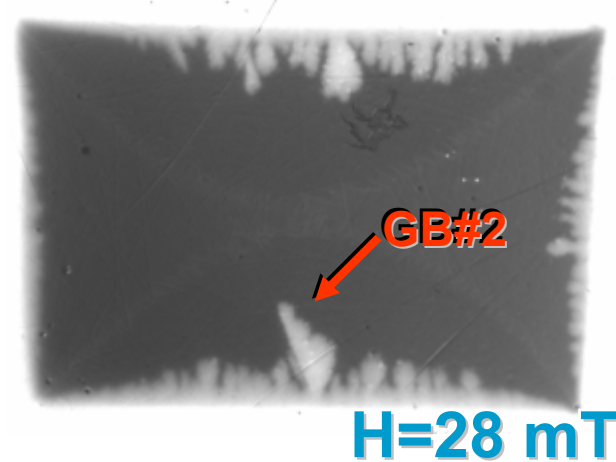
Sample thickness reduced to 0.3 mm



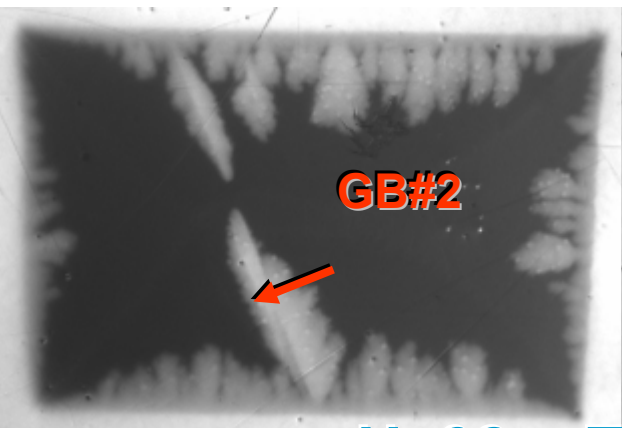
H=24 mT



H=26 mT

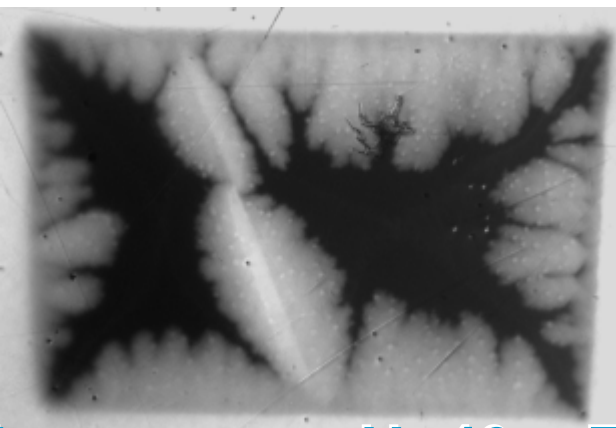


H=28 mT



GB#2

H=32 mT



H=40 mT



GB#2

H=0 FC T=6 K

1 mm

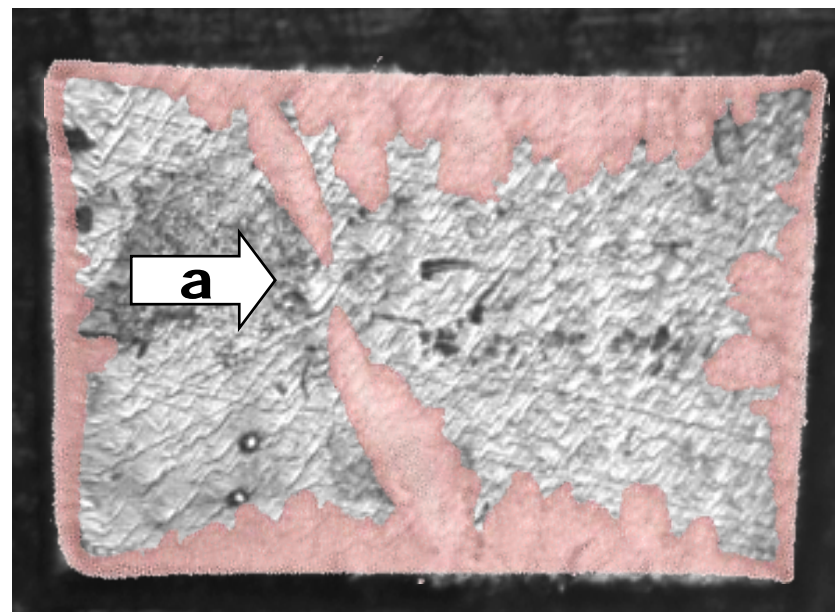
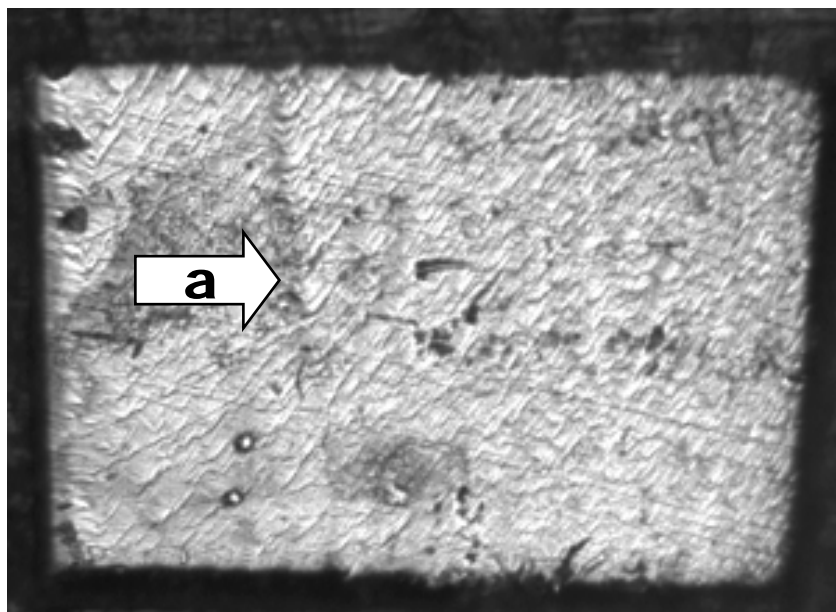
T=6 K

Now flux penetrates the GB from both sides
-GB acts as weak link in both ZFC and FC states.



But this sample is rough!

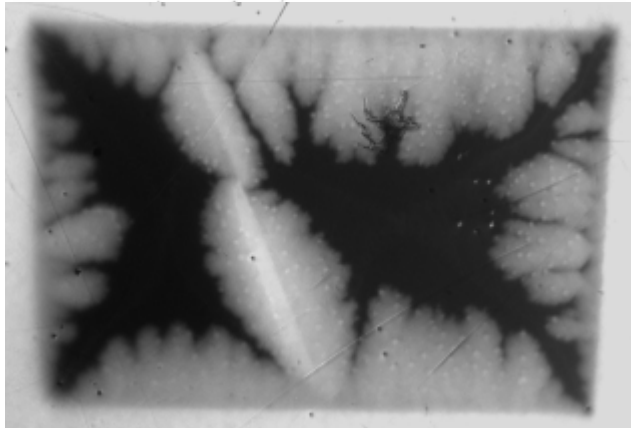
- Surface has considerable roughness from cutting and a groove (a) that crosses the GB.



H=32 mT penetration
superimposed on surface



Conclusions from Experiment 2



H=0 FC T=6 K

- 🌐 Explanation for asymmetric flux penetration and the absence of MO contrast in FC in Expt. 1:
 - 🌐 High sensitivity to angle between GB and direction to externally applied field.
- 🌐 Study of flux penetration along GB#2 in thin samples, when GB perpendicular to surface, shows weak link in *both* FC and ZFC.

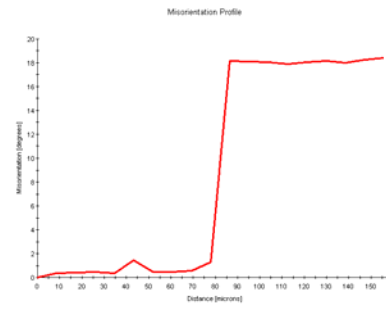
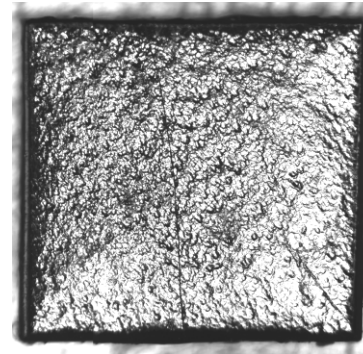
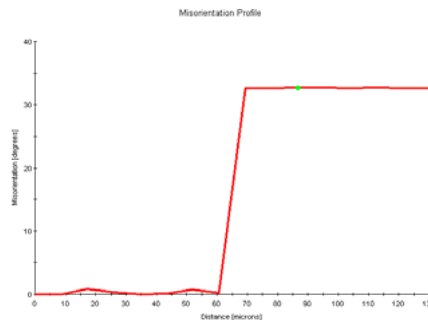
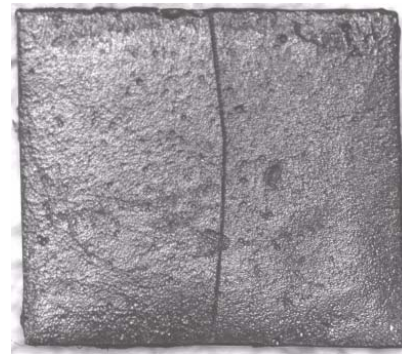


Microstructure of the Grain Boundaries

1. Crystallographic disorientation measured using OIM in FESEM.

- Penetration GBs had angular disorientations of 17.8° (SRF'05 perpendicular) and 32.7° (rotated sample this presentation)

GB#1 (normal-to-surface) disorientation angle between grains $\approx 17.8^\circ$
Orientation Imaging Microscopy (OIM): by D. Abraimov



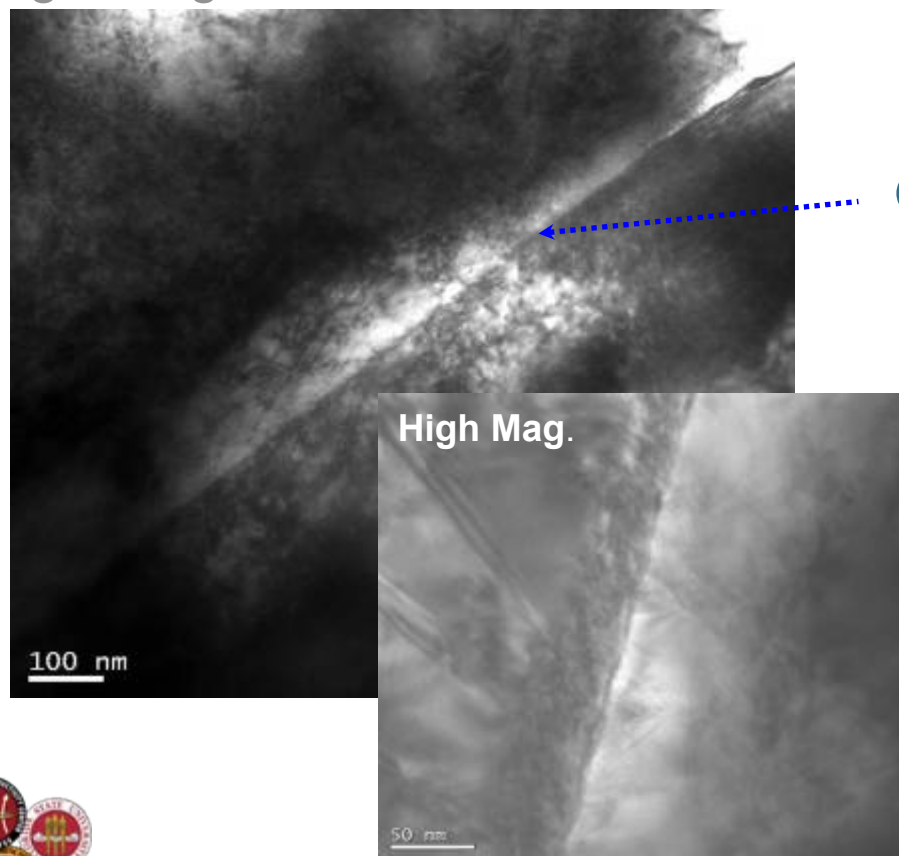
GB#2 (originally 35° to surface) disorientation angle between grains $\approx 32.7^\circ$
Orientation Imaging Microscopy (OIM): by D. Abraimov



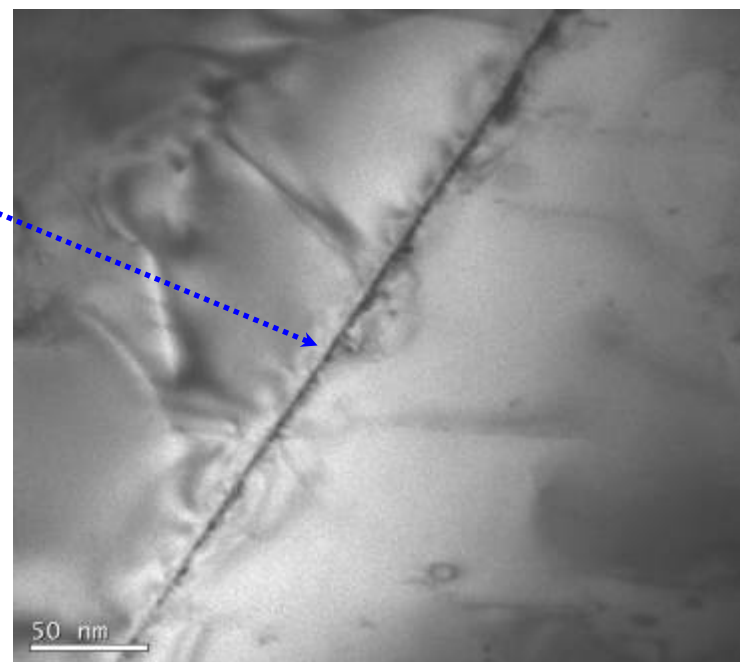
2. Microstructure by TEM

GB1 (SRF'05 “weak” GB): TEM

Sample A: Ground to $\sim 10\ \mu\text{m}$ thick then finish with BCP: Dense dislocation networks remain from grinding.



Sample B: Mechanical polishing stopped at $\sim 20\ \mu\text{m}$. Then finish with BCP.

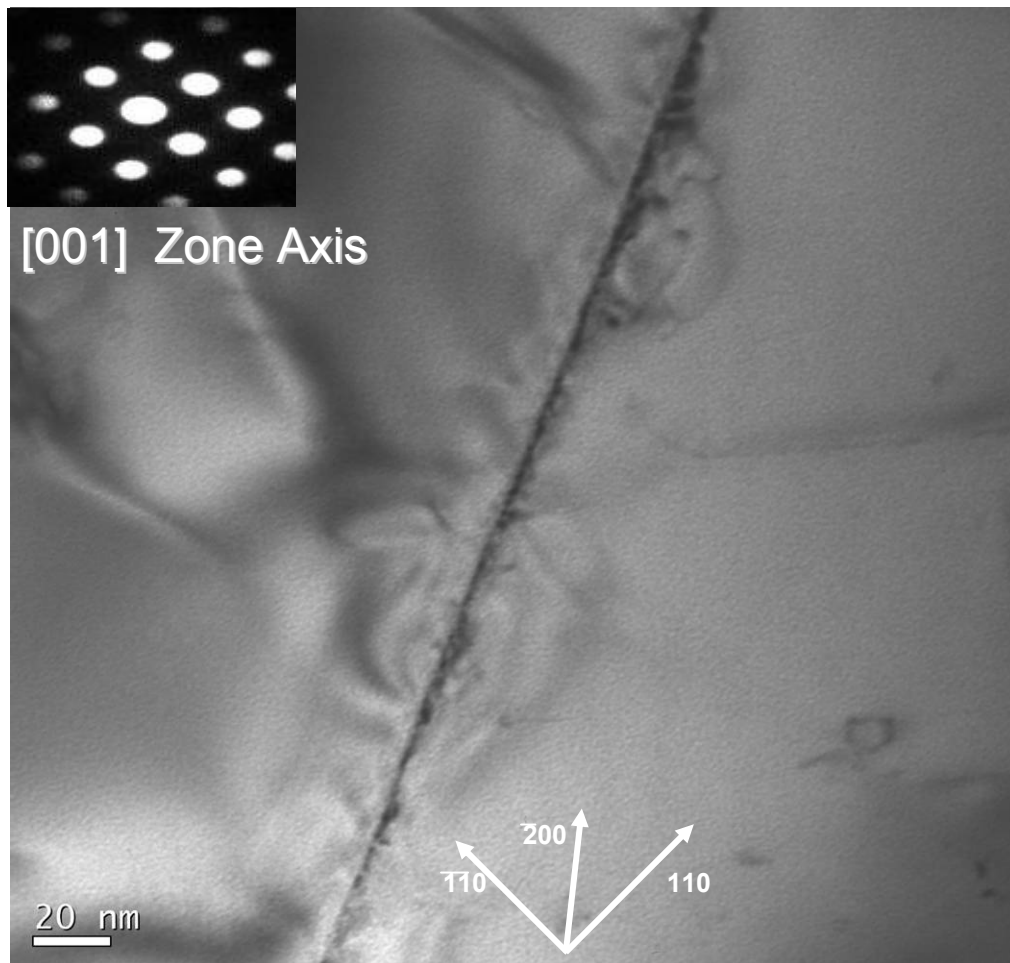


TEM Bright Field Image

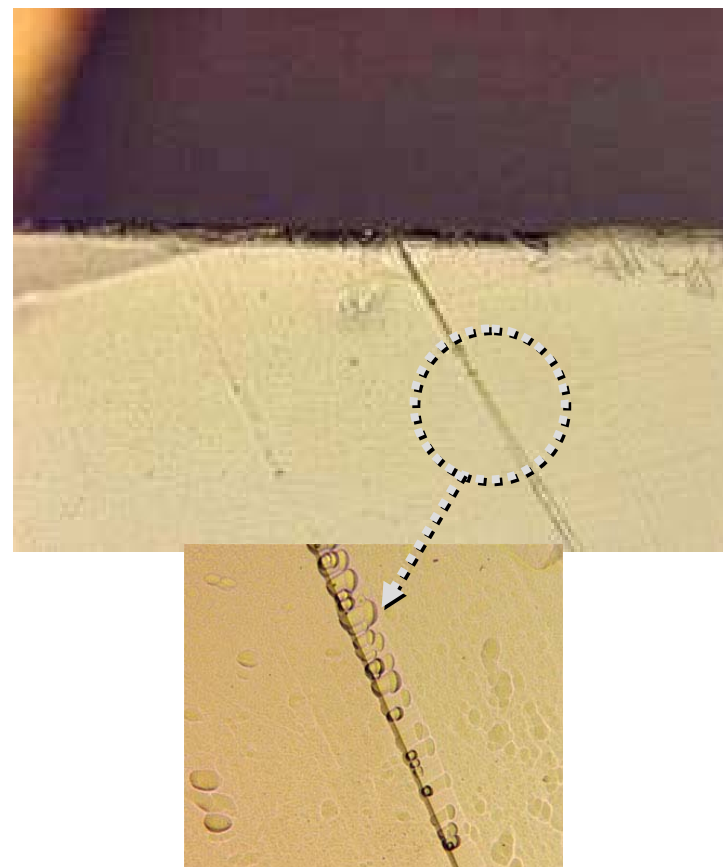
Z. H. Sung



BCP Can Produce Very Good TEM Foils



Light Microscope Overview



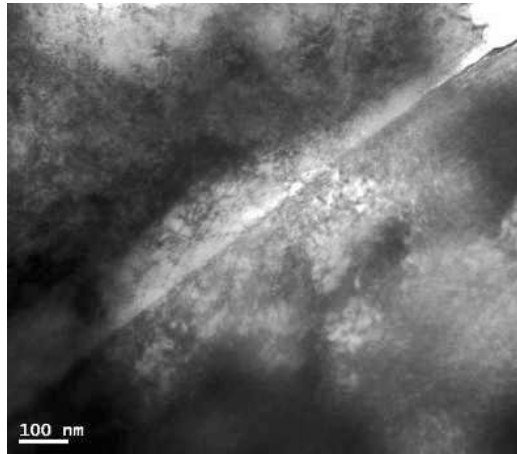
Z. H. Sung

Uniform transmission contrast indicates
no step at GB

There is always some
preferential BCP removal at GBs

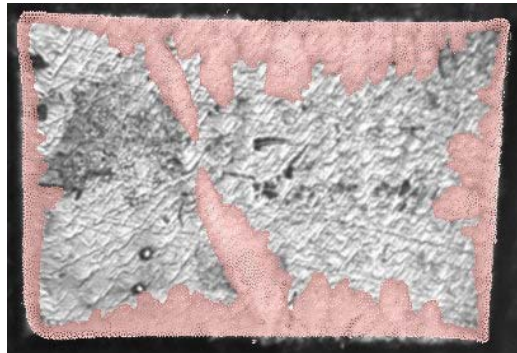


Surface Cold Work and Removal



- With only $<5 \mu\text{m}$ removed by BCP there remains a dense dislocation array left by the grinding action of the polishing grit.

- For the diamond-saw slices and mechanically polished surfaces of GB#2 in this presentation there will also have been a high density of dislocations, again to at least $5 \mu\text{m}$ in depth.



BCP can produce zero-step and minimal groove topology.

- 🌐 In order to be able to produce an electron transparent TEM foil of the GB there must be little or no step or groove created at the GB.
 - 🌐 Careful mechanical polishing followed by $<10\mu\text{m}$ surface removal by BCP creates this condition here.
- 🌐 Polishing Recipe used for TEM sample in previous slide:
 - 🌐 1. Flatten the sample surface with 400 grit SiC paper
 - 2. Decrease the sample thickness with 600 grit SiC paper ($14\ \mu\text{m}$), removing $\sim 500\ \mu\text{m}$ from each surface.
 - 3. Polish with 800 grit SiC paper ($10\ \mu\text{m}$)
 - 4. Final Sandpaper grit is 1200 ($5\ \mu\text{m}$)
 - 5. Use very low-force “Mini-Met” polisher with Alumina powders ($1\ \mu\text{m}$ followed by $0.3\ \mu\text{m}$)
The final step takes about 1 and half hour to remove all of scratches.

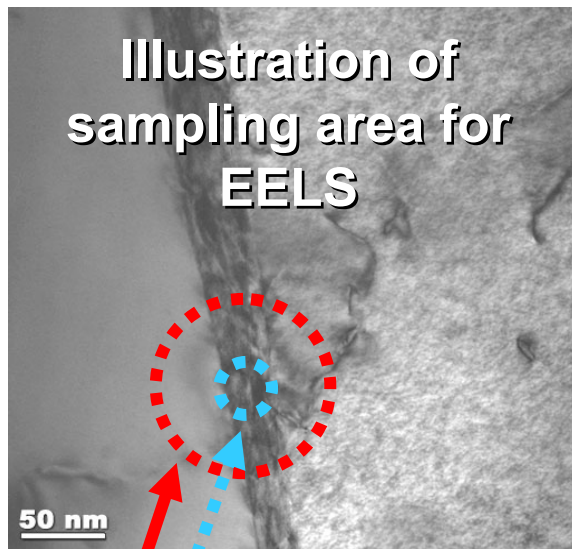
Note: Note: All SiC-paper steps performed *dry* – as this reduces embedding of SiC into sample surface.

Z. H. Sung



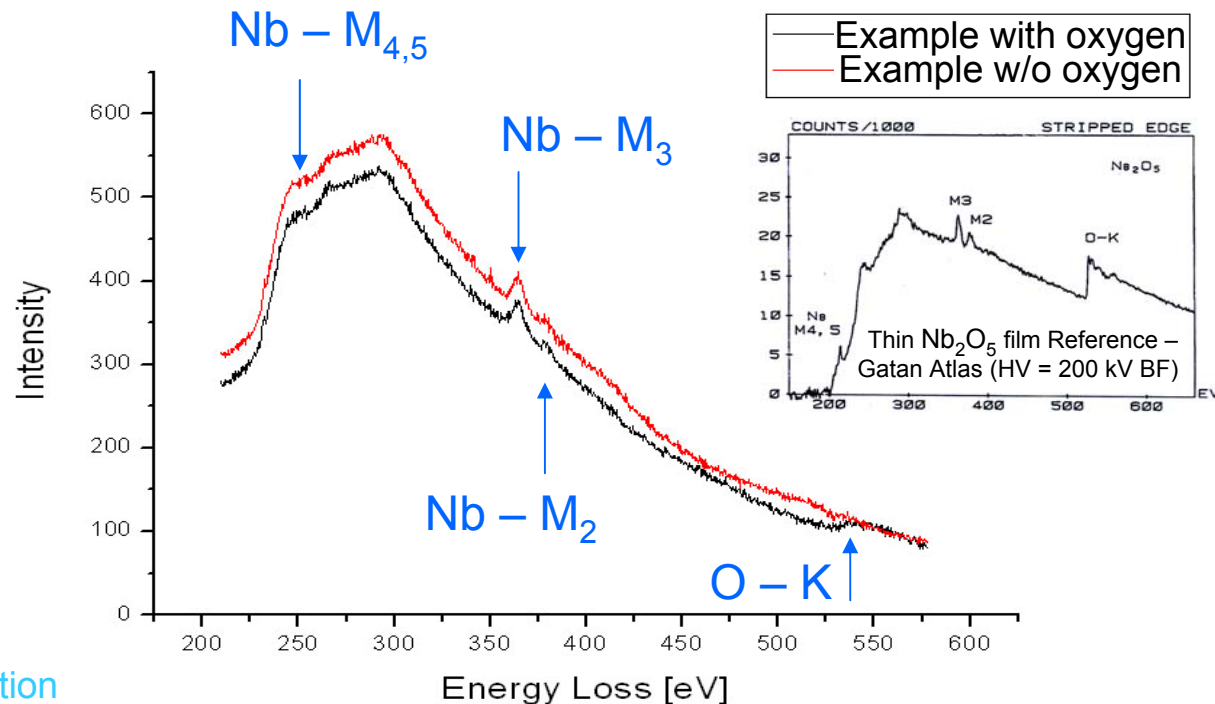
Grain Boundary Chemistry: Electron Energy Loss Spectroscopy in TEM

- Successful GB TEM foils allow us to perform μ -chemical comparisons between the GB region and the Grain.



Spectrometer entrance aperture position (diaphragm : ~100nm)

Energy loss spectrum position



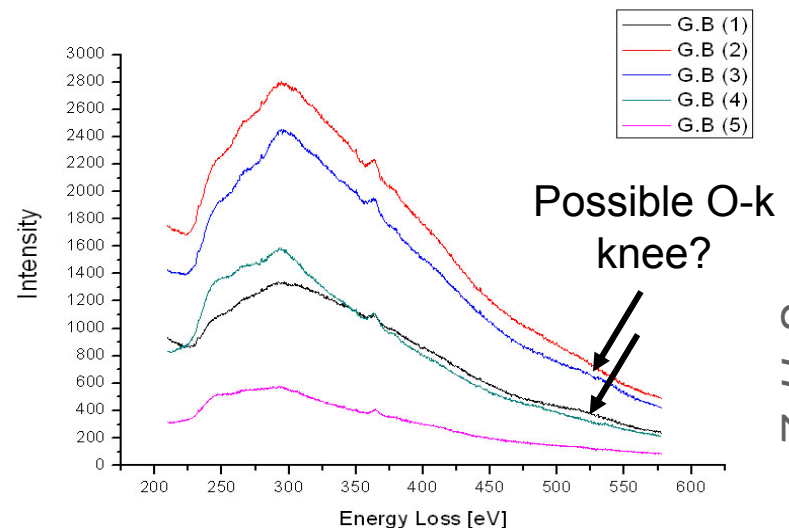
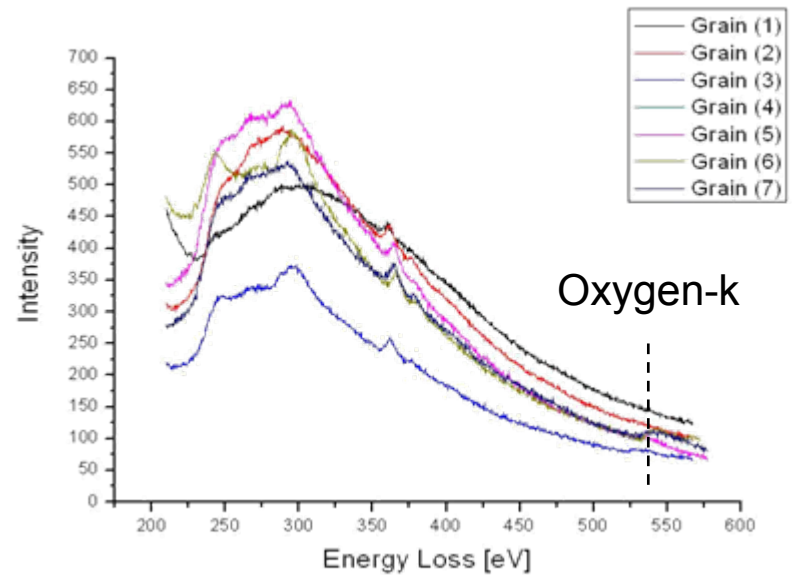
Location of peaks in example analyses with and without oxygen

Z. H. Sung



Summary of Multiple EELS Analyses

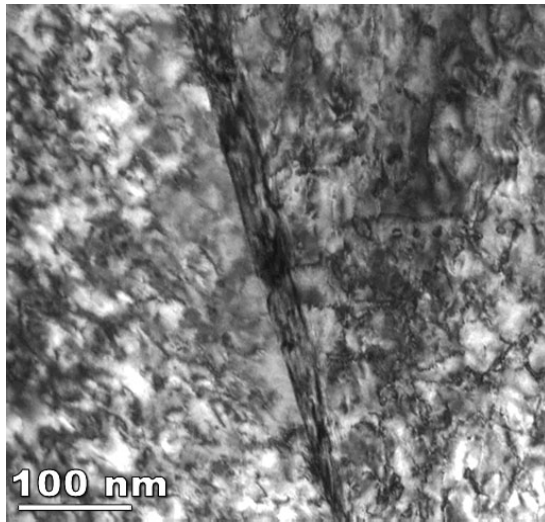
- 🌐 Oxygen-K peak detectable in about 80% of in-grain regions (50-20 μm away from GB).
- 🌐 Oxygen peak (K shell) not clearly visible in 100 nm diameter grain boundary analysis regions.
- 🌐 Note: *All* surfaces will have some Nb oxide – so that level of oxygen is not being detected in these traces.



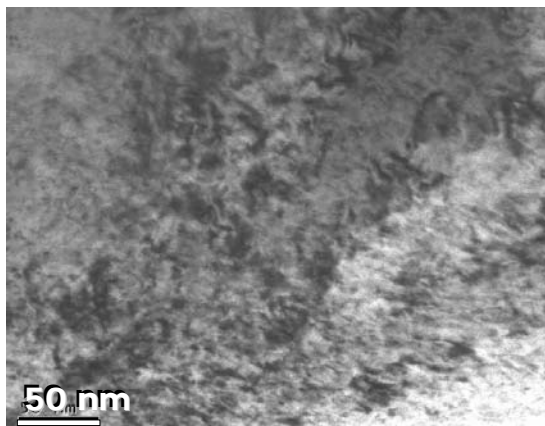
Z. H. Sung



Ar Ion Milling and FIB'ing Can Introduce Defects



- **Low angle Ar ion milling introduced dislocation & point defects** (TEM Image left: Ar+ 2.5 kV, 5 mA, 8° tilt, 10 min)



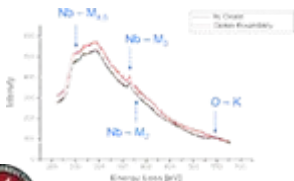
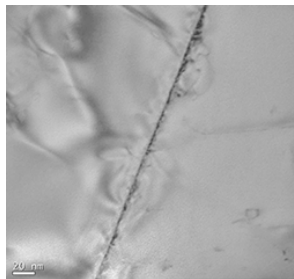
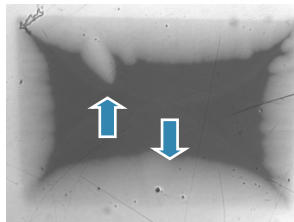
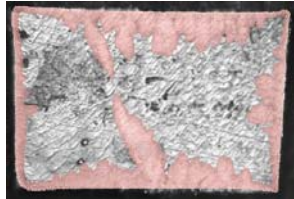
- **Focused Ion Beam:** produced very good foils for EELS but evidence for point defect/ion embedding damage.

Z. H. Sung



Summary

- MOI reveals weakness in the grain boundaries of the as-received large grain slice that is not explained by topology.
- However, that weakness is only revealed when the grain boundary is close to parallel with the applied magnetic field.
- For randomly oriented sheet in an RF cavity, the larger the grains the greater the distance between these weak GB locations but the greater the length of weak GB at that location.
- Using TEM preparation techniques followed by BCP perfectly flat sample surfaces.
- EELS consistently shows oxygen in grains away from GB *but* within 50 nm of GB the oxygen signal falls below detectable levels.



Acknowledgments

- **Very large grain Nb slice provided to Applied Superconductivity Center by Peter Kneisel at the Thomas Jefferson National Accelerator Facility.**
- **OIM was performed by Dmytro Abraimov.**
- **Support for this work at the UW-ASC was through the DOE-LCRD under grant DE-FG02-05ER41392.**

